Wasit Journal of Engineering Sciences

Journal homepage: https://ejuow.uowasit.edu.iq

3D Buildings Change Detection from Aerial and Satellite Stereo Imagery Using Kullback–Leibler Divergence Algorithm

Sitav H. Abdullah[1 *], Haval A. Sadeq [2], Dleen M. Salih[2]

Affiliations
[1] Construction & Materials Technology Engineering Department, Erbil Technology college/EPU;
[2] Geomatics (Surveying) Engineering Department, College of Engineering, Salahaddin University-Erbil

Correspondence
sitav.abdullah@el.epu.edu.iq

Accepted
20/12/2022

Doi
10.31185/ejuow.Vol10.Iss4.454

Abstract

Monitoring city sprawls is considered an essential subject in urban planning. The most important object in the urban areas is the building; therefore, finding an automatic method for detecting the changes in the buildings is considered a priority task for researchers to consider the changes in a district, especially for assessing the damages during disasters and updating geo-database. However, using 2D images to detect changes is ineffective because of the various imaging environments and the parameters of the sensors. Furthermore, during the change detection process, it is difficult to distinguish between the building and other objects due to the similarity of spectral properties. Therefore, it is necessary to use stereo images for DSM generation and then find the changes. This paper proposes a Kullback–Leibler divergence (KLD) algorithm to detect urban area changes based on stereo imagery. Two DSMs have been obtained through the photogrammetric process using two different sensors. The first data set is based on the stereo aerial imagery captured in 2012 and the second stereo is from the worldview-2 sensor captured in 2017. Before applying the KLD algorithm, the aerial's DSM, which has an original resolution of 0.3m, was resampled to 1 m to make it similar to the satellite's DSM. Three study areas have been selected for the algorithms test, located in Erbil-Iraq. The assessment shows that the KLD detected changes better than other methods after removing the small fragments through the post-processing step. For the evaluation, the confusion matrix has been determined for each study area. The analysis demonstrates that the overall accuracy for the three study areas where 89.3%, 91.1% and 88.9 %, respectively.

Keywords: Power transformer; solar radiation; heat transfer; fin geometry

الخلاصة: تعتبر مراقبة امتداد المدينة موضوعًا أساسيًا في التخطيط الحضري. أهم شيء في المناطق الحضرية هو المبنى. لذلك ، فإن العثور على طريقة تلقائية لاكتشاف التغييرات في المباني يعتبر مهمة ذات أولوية للباحثين للنظر في التغييرات في المنطقة ، وخاصة لتقييم الأضرار أثناء الكوارث وتحديث قاعدة البيانات الجغرافية. ومع ذلك ، فإن استخدام الصور ثنائية الأبعاد لاكتشاف التغييرات غير فعال بسبب بيئات التصوير المختلفة ومعلمات أجهزة الاستشعار. علاوة على ذلك ، أثناء عملية الكشف عن التغيير ، من الصعب التمييز بين المبنى والأشياء الأخرى بسبب تشابه الخصائص الطيفية. لذلك ، من الضروري استخدام الصور المجسمة لتوليد DSM ثم البحث عن التغييرات. تقترح هذه الورقة خوارزمية Kullback – Leibler divergence (KLD) لاكتشاف التغيرات في المناطق الحضرية بناءً على الصور المجسمة. تم الحصول على اثنين من DSM من خلال عملية القياس التصويري باستخدام جهازي استشعار مختلفين. تعتمد مجموعة البيانات الأولى على

الصور الجوية الاستريو التي تم التقاطها في عام 2012 والثاني من مستشعر الرؤية العالمية -2 الذي تم التقاطه في عام 2017. قبل تطبيق خوارزمية KLD ، تمت إعادة أخذ عينات DSM للهوائي ، والتي تبلغ دقتها الأصلية 0.3 م. إلى 1 متر لجعله مشابهًا لـ DSM للقمر الصناعي. تم اختيار ثلاث مناطق دراسية لاختبار الخوارزميات ، وتقع في أربيل - العراق. يوضح التقييم أن KLD اكتشف التغييرات بشكل أفضل من الطرق الأخرى بعد إزالة الأجزاء الصغيرة من خلال خطوة ما بعد المعالجة. للتقييم ، تم تحديد مصفوفة الارتباك لكل منطقة دراسة. أوضح التحليل أن الدقة الكلية لمناطق الدراسة الثلاث حيث 89.3٪ ، 91.1٪ و 88.9٪ على التوالي.

1. INTRODUCTION

Monitoring Change detection of buildings is considered to be very significant for the decision-makers. It provides necessary information that helps to assess the changes in various applications such as disaster assessment, urban planning, cadastral map updating, and others. Although manually detecting the changes is considered very accurate and reliable but is considered to be very time-consuming and expensive. Therefore, the trend is currently focusing on the automatic and semiautomatic methods since it has proven the result rapidly. Generally, aerial or satellite imagery change detection can be classified into 2D and 3D change detection [1]. The common change detection techniques were dominated by 2D image-based algorithms based on pixel intensity analysis of the imagery using radiometric values [1-6]. In addition to applying changes detection to the urban area, it has been widely used to monitor the changes in the vegetation and observer the cultivation [7, 8]. On the other hand, various studies have been conducted using DSMs for change detection based on using 3D features of the objects [9-13]. Also, the combination of the 2D and 3D features has been approved to give good results in change detection to detect the changes by monitoring the newly constructed objects Huang [14].

However, from the above studies, it can be noticed many limitations will lead to minimising the detection accuracies, such as threshold values. It has been noticed that selecting the optimal threshold value is considered a challenge in the image detection method, and it has directly related to the amount of detected change in the pixels. Furthermore, important information will be omitted during the change detection process, due to the spatial relations between the neighbourhood of the pixel have not been taken into consideration [15]. However, an alternative method to solve the above limitation is to use object-based and information-based techniques. For instance, the information-based algorithm, the Kullback-Leibler Divergence method, is based on detecting the similarity between two probability density functions(PDF), which can be used in change detection [16].

Based on the literature, none of the studies is focused on using DSM in change detection using two different sensors (i.e. detecting the changes between the aerial and satellite data). Therefore, this study addresses the changes from different sensors using Kullback Leibler Divergence.

The structure of the paper is as follows, the introduction in this section. The applied methodology and used datasets are described in section 2. In section 3, the experiments have been illustrated, and the result evaluation has also been presented. In section 4, the discussion of the applied method has been presented. Finally, the conclusion and future improvement have been presented in section 5.

2. METHODOLOGY AND USED DATASETS

2.1. STUDY AREA AND DATASETS

An area of 5x5 km square with significant urban development in Erbil city is selected and acquired for the study. Within the study area, the methodology is evaluated in three different test areas: Area 1 (Ankawa), Area 2 (Dream City) and Area 3 ((sarbasty (32 park)). There are two groups of data in the data set: the first one is stereo satellite imagery from the world view-02 (WV02) sensor, captured in 2017 with a 0.5m GSD resolution as shown in Figure 1, while the second set is aerial imagery of Erbil city acquired in 2012 with a 0.10m GSD resolution by using an Ultracam Xp sensor. The Aerial images were provided by Salahaddin University's Geomatics (Surveying) Engineering Department.

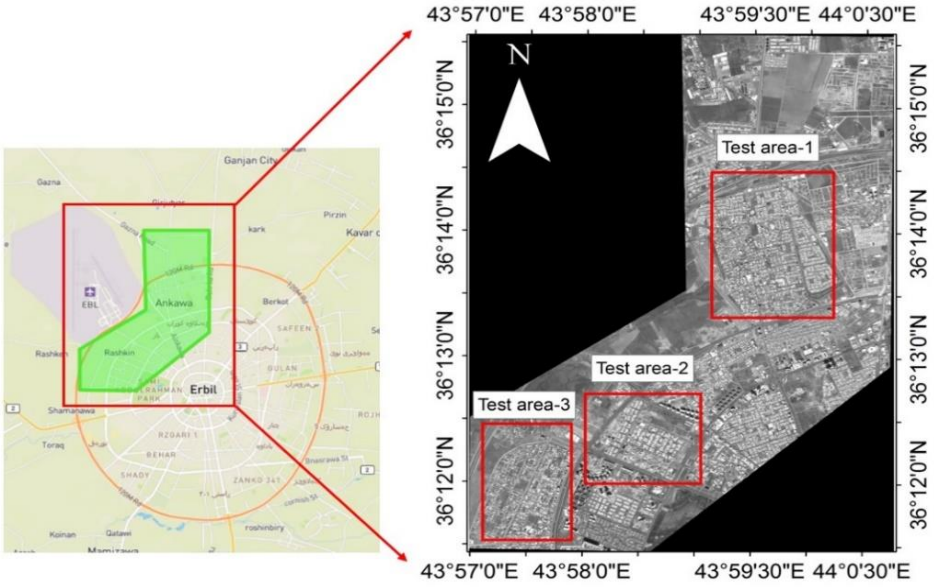

Figure 1 The location of the three test areas on the VHR Stereo satellite imagery

2.2. Measuring Ground Control Points (GCPs)

For the purpose of processing the satellite and aerial images, Also for evaluating the accuracy of generated DSMs, a set of GCPs was measured by using a Leica-1200 GPS instrument. Through the use of the GPS post-processing kinematics (PPK) technique, the GCPs were observed. During the observation, a measurement was taken consciously at the base station for seven hours, and the required observation for each rover station was approximately three minutes.

The GCPs were acquired based on the projection Universal Transverse Mercator (UTM) zone 38N and datum WGS 84 ellipsoid. Afterwards, the GPS data was imported to the Leica geo-office software for post-processing purposes, and they were processed according to the nearest Continuously Operating Reference Station (CORS), which was based in Iraq Survey Erbil (ISER) as a source of GPS corrections. The result relative to the base station was thirty GCPs within millimetres accuracy.

2.3. The Reference Data

It is necessary to collect accurate ground truth, or reference data in order to assess the accuracy of a method, and also to determine a method's suitability and efficiency (Tian, 2013). In this research, the reference data was prepared for each study area by manual compilation of the buildings using summit evolution software. The stereo Aerial and satellite images were added and processed to extract boundaries of all changed and unchanged buildings, then the digitized reference data are imported to the GIS software (ESRI, Arc Map 10) for area computation of each changed and unchanged building. The computed reference data (shown in Figure 2 where the changed buildings are highlighted in Green) will be used for evaluating the accuracy of change detection algorithms.

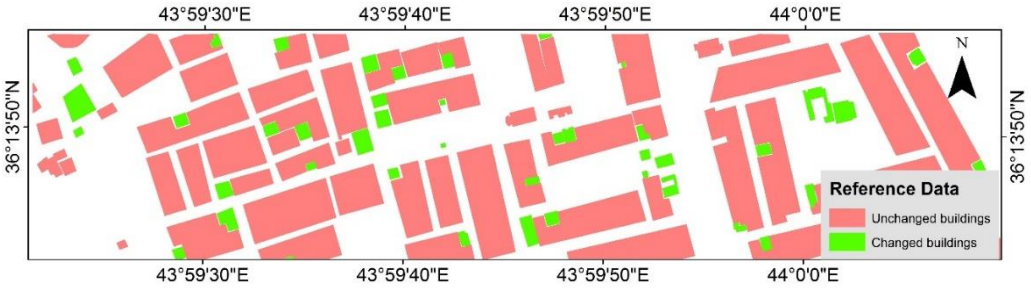

a-test area one

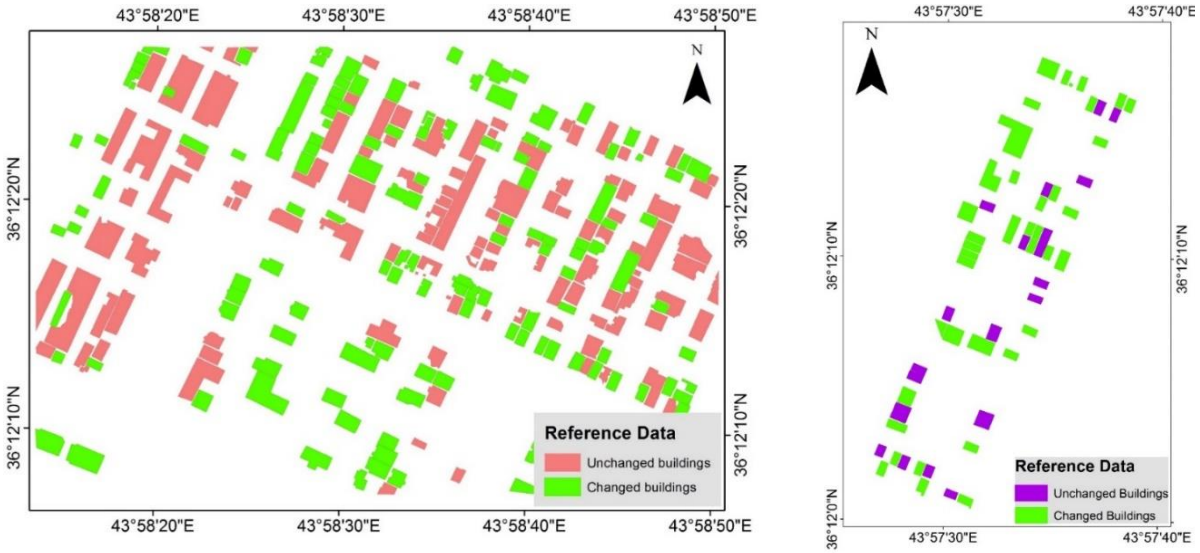

b-test area two c- test area three

Figure 2 Computed reference data: for a) test area one, b) test area two and c) test area three

2.4.Applying Change Detection

In this research, the KL-Divergence change detection algorithm has been used to identify the changes. The flow chart of the proposed building change detection methodology is presented in Figure 3. Initially, the stereo aerial and satellite images are used to generate the DSMs. Afterwards, the DSMs are used to apply the KL-Divergence algorithm for detecting 3D building changes.

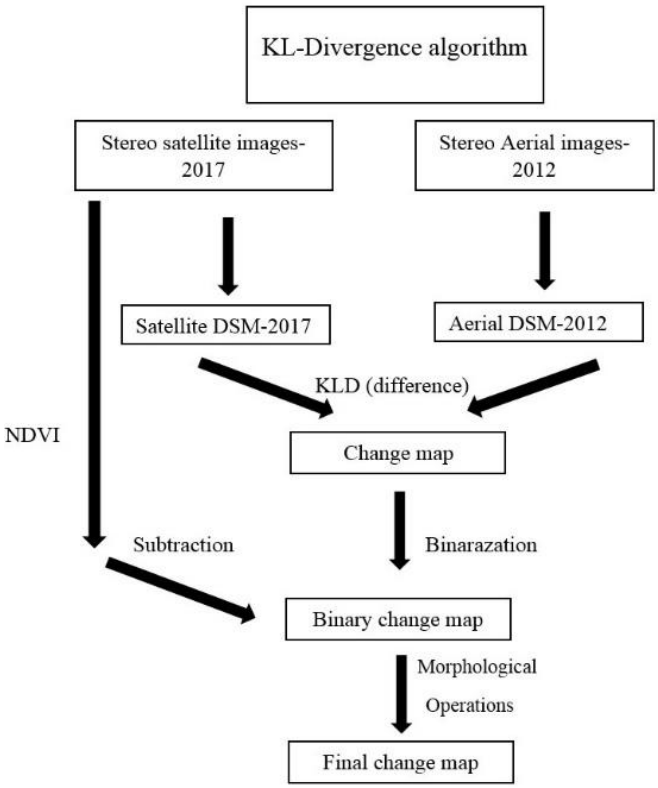

Figure 3 General workflow of information-based KL-Divergence method that has been implemented in this research.

2.4.1. Data Processing and DSM Generation

In this study, ERDAS Imagine software is used to process the stereo aerial and satellite images. The DSMs are generated by the image matching process using the least square matching algorithm.
The least squares matching (LSM) algorithm minimizes gray value differences between the reference window and search window through an adjustment process, in which geometric (location, size, and shape of the search window) and radiometric (pixel gray values) corrections are determined for each matching window based on the affine transformation parmaters [17].

Generally, DSM co-registration is necessary before applying any change detection method to avoid false change detection caused by image displacement [1]. However, In the framework of this research, no image registration techniques were required, because the data sets have been derived using the same GCPs during the processing of the stereo images either from aerial or satellite sensors, for the purpose of producing DSMs and ortho-imagery.

2.4.2. Applying Kullback Leibler Divergence

KL divergence is a fundamental equation of information theory that measures a statistical similarity between the shapes of two probability distribution functions (PDFs), which has been applied widely in theory and practice fields [18]. The higher the similarity between the two PDFs, the lower the divergence.
Assuming P(x) and Q(x) are two probability density functions. The KL-Divergence can assess the divergence between these two probability density functions as follow :

$$KL(P \parallel Q) = \sum_{x \in X} P(x) \log\left(\frac{P(x)}{Q(x)}\right) = \int_{-\infty}^{\infty} P(x) \log\left(\frac{P(x)}{Q(x)}\right) dx \quad (1)$$

In case if the two probability density functions are close to each other, the Kullback–Leibler divergence is small. In contrast, it is larger if there is a great deviation between them [19]. The KLD is always non-negative and equals zero only if the two distributions are identical.
In this research, for applying the KL-Divergence algorithm on generated DSMs, a specific code written in the MATLAB programming platform has been used. First, the Probability Density Functions (PDF)s of the pixel values are generated; then, the KL-Divergence of the PDFs are calculated as a measure of change, Afterwards, The obtained result after applying KLD was converted into the binary change map.
However, some virtual changes that do not belong to the buildings have appeared as object differences also, which theys are removed through the following steps.
Step 1) Elimination of the Vegetation
Since the main focus of this research is only on detecting the changes in the buildings, therefore the elimination of the vegetation from the 3D change detection scheme is essential. To separate the changes in the buildings from vegetation, the NDVI masks have been computed from the near-infrared and visible light reflected from stereo satellite images as it is given in equation (2).

$$NDVI = (NIR — RED) / (NIR + RED) \quad (2)$$

Where: NIR and VIS stand for the spectral reflectance measurements acquired in the near-infrared and RED bands , respectively.
Then NDVI mask was subtracted from the binary change map. Later, the vegetation was removed from the change map. But Spurious change in altitude can also be caused by other land covers or DSM computation errors displayed around the buildings that affected Building change extraction results. Therefore, more adaptive post-processing steps are required to keep only the real changes in the buildings.
Step 2) Applying Mathematical Morphology
Spurious detected changes that are displayed as objects around the buildings need to be removed by applying some mathematical morphology(MM) operations, which are known as an opening followed by a closing operation. MM is a non-linear process that is commonly used in image analysis which is based on modifying the geometrical shapes within the image, rather than pixel values [20]. The basic morphological operations that are introduced are erosion; dilation; opening and closing.
Erosion and dilation are the simplest operations in mathematical morphology. In practice, dilations and erosions are usually employed in pairs [21]. The result of the dilation and erosion combination is called opening or closing depending on which is applied first.
In this research, MATLAB software has been used for the purpose of applying (opening and closing) operations.

3. EXPERIMENT AND RESULT EVALUATION

In this section, the proposed methodology in section 2 for 3D building change detection is performed. It is started with generation of DSM models from both aerial and satellite imagery followed by applying KL-divergence algorithm for building change detection and ended by evaluate/assess the produced results. Hence, results and their assessment have been reported in this paper as two following main sub-section.

3.1. DSM generation Evaluation

Photogrammetric approach has been used to generate DSM from both aerial and satellite imagery, Figure (4) presents the generated DSM result for three selected study areas. Basically, generation procedure is done by the image matching process using least square (LS) matching algorithm. Furthermore, a particular strategy has been conducted in setting the main parameters of the software such as: identifying the window size and correlation coefficient for image matching threshold value determination. It is important to mention that the topographic category type has been set as a (flat area) due to the location of the study area which is an urban area without rolling or hills. (note: I haven't included the details of setting those parameters as it was mentioned in the thesis because of the no. of pages limitation)

As a result, two DSMs with 0.3m and 1m grid cell size from aerial photograph and satellite image respectively have been generated for all selected study areas (Figure 4 (a, c and e) presents the aerial-DSM for test area one, two and three respectively, while (b, d and f) presents the satellite-DSMs for the corresponding areas). basically, both generated DSM as a multiple raster datasets should be stored with the same cell resolution. Hence, the produced DSM from aerial images were resampled to 1 m grid cell size in order to have the same cell resolution with the one that generated from satellite image. As this study is focusing on 3D Building changes (i.e height change detection), Nearest neighbor technique is the method that has been conducted in resampling procedure because this method will keep the elevation values from the input raster dataset. That means the closest center in the output raster product is determined by the center from the input raster data, which in turn means no changing in the elevation values will produce.

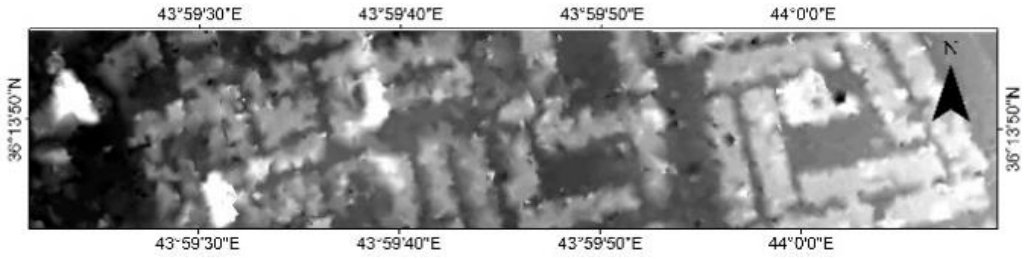

a- test area one

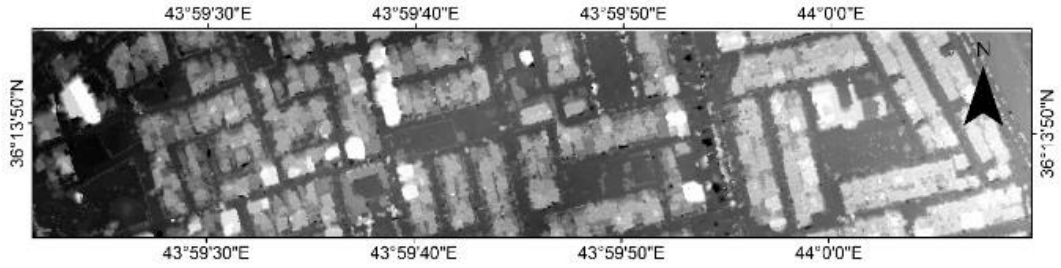

b- test area one

c-test area two

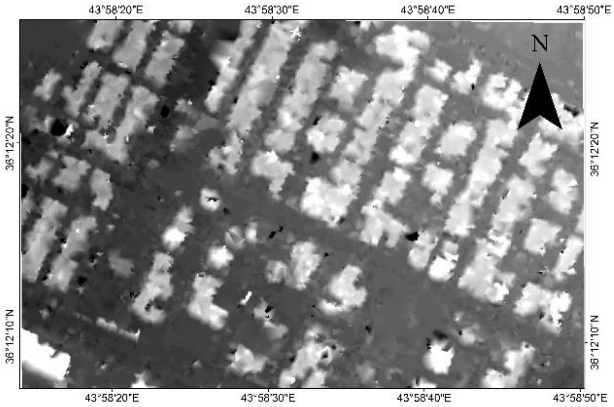

d-test area two

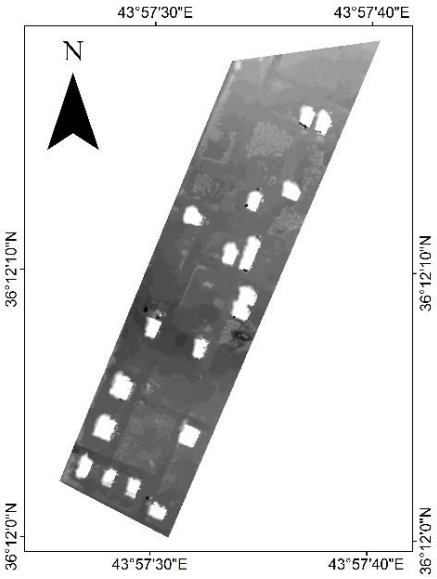

e- test area three

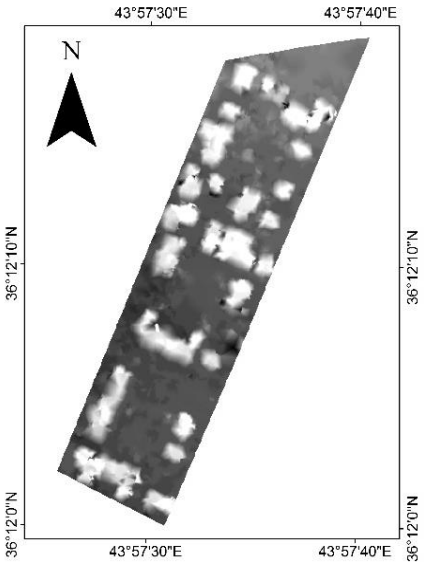

f- test area three

Figure 4 The generated DSMs For all Test areas

As an accuracy assessment step and due to that this research is relevant to the height difference, the vertical accuracy assessment of the generated DSMs is conducted. Vertical Root-Mean-Square-Error (RMSE) formula used as a comparative scale between the computed Z-coordinate values at checkpoints with the same points on generated DSMs.

$$\mathrm{RMSE} = \pm\sqrt{\frac{1}{n}\sum_{i=1}^{n} e_{\upsilon i}^{2}} \qquad (3)$$

$$e_{\upsilon i} = \upsilon_{ri} - e_{mi}$$

Where;

RMSE = root mean square error,

υ_{ri} = reference (checkpoint) elevation at the point i,

e_{mi} = DSM elevation at the point i,

n = the number of ground checkpoints.

The detailed point accuracy information is shown in Table 1.

Table 1 Result of vertical Accuracy Assessments of the DSMs Extracted by Checkpoints

Data source	Test area	Checkpoint (CP) ID	Checkpoint elevation	Extracted elevation from DSM	Difference (m)	RMSE (m)
DSM from Satellite images	Test area -1	CP 23	424.5247	425.6534	1.1287	0.9399
		CP 25	426.5007	427.0588	0.5581	
		CP 29	430.1561	431.1958	1.0397	
		CP 30	429.5691	430.5004	0.9313	
	Test area -2	CP 1	407.7313	409.0902	1.3589	1.0987
		CP 2	408.4806	409.0874	0.6068	
		CP 10	411.0869	411.9852	0.8983	
		CP 11	407.2184	408.4309	1.2125	
		CP 31	409.2837	410.4879	1.2425	
	Test area -3	CP 1	407.7313	408.1491	0.4178	0.4762
		CP 7	408.3031	408.7008	0.3977	
		CP 14	403.0201	403.3124	0.2923	
		CP 17	397.3475	397.7364	0.3889	
		CP 20	405.156	405.9074	0.7514	
DSM from Aerial images	Test area -1	CP 23	424.5247	424.7710	0.2463	0.2275
		CP 24	426.5007	426.6972	0.1965	
		CP32	428.7845	428.9854	0.2009	
		CP33	422.7417	423.0029	0.2612	
		CP34	424.0978	424.2701	0.1723	
		CP35	423.3759	423.6460	0.2701	
	Test area -2	CP 3	409.9875	409.9245	0.0630	0.2947
		CP 5	410.3585	409.9349	0.4236	
		CP 6	411.7181	411.4197	0.2984	
		CP36	408.3021	407.9230	0.3791	
		CP37	409.0528	408.7592	0.2936	
		CP38	411.8407	411.7035	0.1372	
	Test area -3	CP 13	402.9905	402.9124	0.0781	0.1826
		CP 14	403.0201	402.7265	0.2936	
		CP 16	401.1738	401.0785	0.0953	
		CP39	406.3641	406.1916	0.1725	
		CP40	403.0426	402.8325	0.2101	
		CP41	405.2287	405.0708	0.1579	

3.2. KL-divergence Evaluation

KL- divergence algorithm applied on generated DSMs via conducting matlab code. Initially, pixel value's PDFs are generated followed by measuring of change through calculating the KL-divergence of those PDFs. Figure (5) presents the obtained results of three tested study areas.

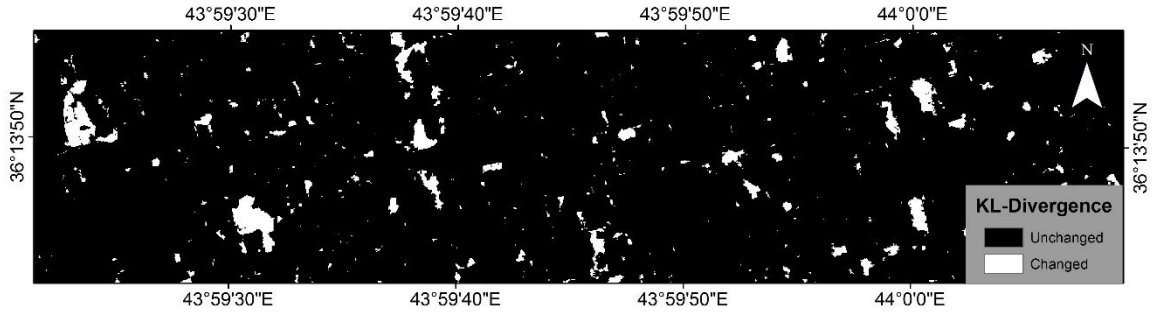

a-test area one

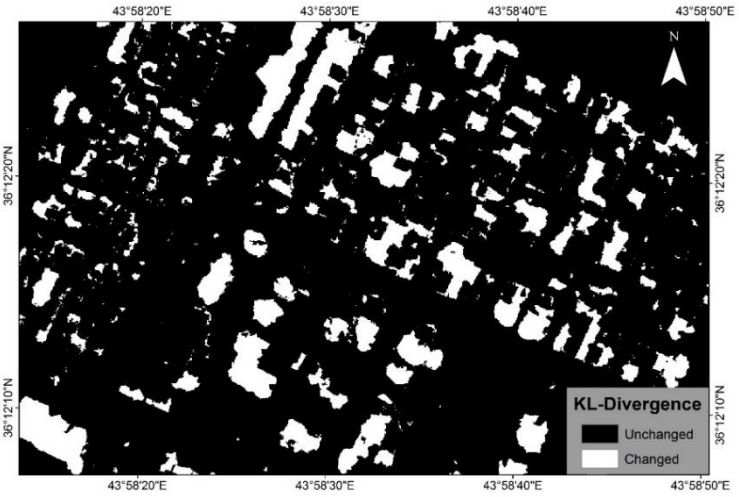

b- test area two

c- test area three

Figure 5 Applied KLD on generated DSMs: for test area one, two and three presented by (a, b and c) respectively.

Those obtained results have converted into the binary change map in order to apply other necessary procedures such as subtracting the NDVI mask to eliminate the vegetation, and also apply mathematical morphology operation to remove pseudo changes that could appear around building. As a result, the noises coming from DSM failures were considerably reduced as can be seen from figure (6).

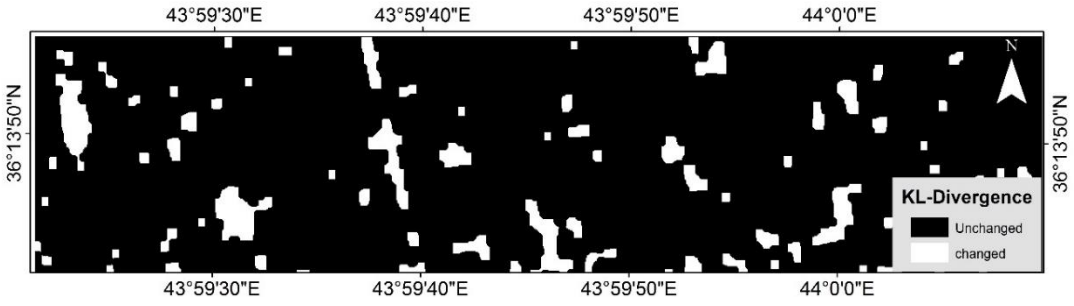

a- test area one

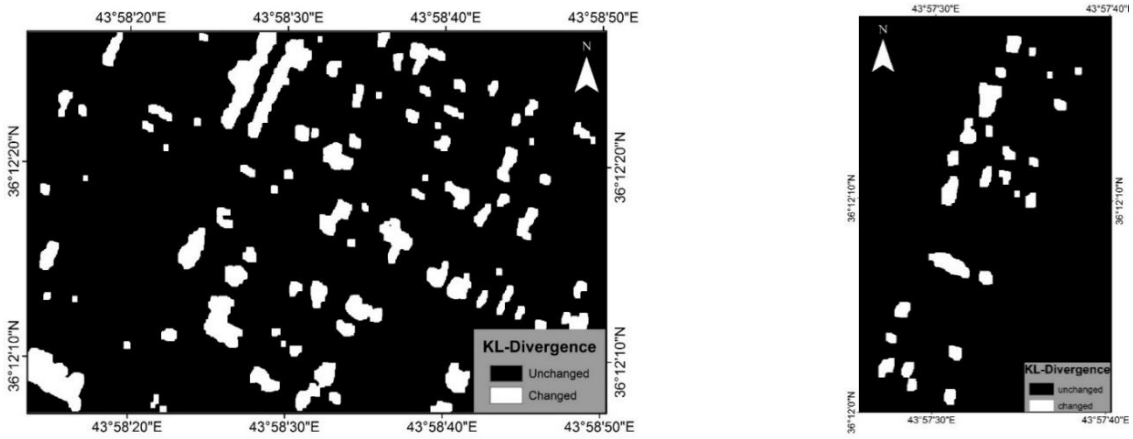

b- test area two c- test area three

Figure 6 The final change map after applying KLD and morphological operations: (a) test area one, (b) test area two and (c) test area three.

In term of accuracy assessment, the effectiveness of the proposed method for the detection of the position and size of the changed buildings and the overall change situation has been evaluated by using confusion matrix for the object based assessment as presented in the Table 2. Basically, the obtained change map is assessed with respect to the reference (ground truth) data. In this assessment method, the changed buildings are treated as single objects without consideration of their shape and size. Only the effectiveness of the detection of distinct changed areas (buildings) in the change map is considered in the evaluation (Tian et al., 2014). Concerning building change detection accuracy, in some cases, the number of correctly detected building are more important.

Table 2 Confusion Matrix – Object Based Assessment

Reference data / **Resultant change map**	**Change**	**No change**
Change	True positive (TP)	False negative(FN)
No change	False positive(FP)	True negative(TN)

In the object-based evaluation, the confusion matrix is based on objects instead of pixels. Therefore, four parameters are measured to assess change detection result.

1. True Positive – the number of changed buildings correctly detected as changed.

2. False Positive – the number of unchanged buildings incorrectly detected as changed.

3. False Negative – the number of changed buildings incorrectly detected as unchanged

4. True Negative – the number of unchanged buildings correctly detected as unchanged.

Several certain quality measures can be derived from the above parameters to assess the performance of a change detection algorithm. Basically, the following quality measures are the most commons:

1) Branching Factor (BF)

The branching factor is the ratio of 'False Positive' and 'True Positive'. It represents the rate at which the incorrect objects are classified by the algorithm as changes.

$$\mathrm{BF} = \frac{\mathrm{FP}}{\mathrm{TP}} \qquad (4)$$

2) Miss Factor (MF)

The miss factor is the ratio of 'False Negative' and 'True Positive'. It represents the rate at which the change objects in the reference data are missed by the algorithm in classification.

$$\mathrm{MF} = \frac{\mathrm{FN}}{\mathrm{TP}} \qquad (5)$$

3) Completeness

Completeness is a quantity measure that defines the proportion of the total number of correctly classified changed objects to the total number of changed objects in the reference data.

$$\text{completeness} = 100 \times \left\{\frac{\mathrm{TP}}{(\mathrm{TP}+\mathrm{FN})}\right\} \qquad (6)$$

Correctness is the fraction of total number of objects correctly identified by the algorithm as changed objects to the total number of changed objects in the reference data. Unlike completeness, it is a significant quality measure shows the correctness of the change detection.

$$\text{Correctness} = 100 \times \left\{\frac{\mathrm{TP}}{(\mathrm{TP}+\mathrm{FP})}\right\} \qquad (7)$$

The ideal values of completeness and correctness are 100%, which means that all changes are correctly identified, and it is achieved when FN = 0 in case of completeness or FP = 0 in case of correctness.

4) Quality Percentage (QP)

The quality percentage is the combination of both completeness and correctness to provide quality percentage for an accuracy measure. The ideal value of QP should be 100%.

$$\mathrm{QP} = 100 \times \left\{\frac{\mathrm{TP}}{(\mathrm{TP}+\mathrm{FP}+\mathrm{FN})}\right\} \qquad (8)$$

5) Overall Accuracy (OA) and Kappa Accuracy (KA):

Overall accuracy is computed by dividing the total correct (i.e., the sum of the major diagonal) by the total number of objects (N) in the error matrix (Tian, 2013).

$$\mathrm{OA} = 100 \times \left\{\frac{\mathrm{TP}+\mathrm{TN}}{\mathrm{N}}\right\} \qquad (9)$$

Overall accuracy alone may create ambiguity, because it takes into account the similar no change objects in both the reference data and the change map while the number of these pixels is presumably very high in most cases, even if one of the classes suffers adversely in classification. Therefore it is suggested to account for other quality assessment parameters for accuracy assessment such as (Varade, 2011).

However, overall accuracy that only takes into consideration the diagonal elements for the ratio in the confusion matrix from table 2, Kappa accuracy considers the non-diagonal elements. Therefore, for the confusion matrix, it is a measure of overall agreement.

Kappa accuracy (KA):

$$\mathrm{KA} = \frac{\mathrm{Pr(a)}-\mathrm{pr(e)}}{1-\mathrm{pr(e)}} \qquad (10)$$

Where: Pr(a) it is calculated in the same way as OA, it is the relative observed agreement between the extracted results and reference data. While

$$\mathrm{pr(e)} = \frac{(\mathrm{TP}+\mathrm{FP})*(\mathrm{TP}+\mathrm{FN})*(\mathrm{FN}+\mathrm{TN})*(\mathrm{FP}+\mathrm{TN})}{\mathrm{N}*\mathrm{N}} \qquad (11)$$

represents the hypothetical probability of the agreement between the extracted result and reference data; N is the total number of observations in confusion matrix (Tian, 2013).

As a result, figure (7) presents the counted change and unchanged buildings in the reference data. Then table (3) and table (4) respectively presents the generated confusion matrix for the tree tested areas and the quality measures that used for analysis purpose.

Figure 7 The red lines are the reference data ,overlain on aerial images to count the number of buildings for accuracy assessment

Table 3 Confusion Matrix for Object-Based Assessment for the Three Test Areas

Result		Confusion matrix		
Change map result /reference data			Change	no change
Test area 1	Kl-divergence	Change No change	31 55	19 586
Test area 2	Kl-divergence	Change No change	153 16	25 269
Test area 3	Kl-divergence	Change No change	43 1	7 21

Table 4 Object Based Quality Assessment for the Data Sets According to (Table 3)

Change map results		**BF**	**MF**	**COMP%**	**COR%**	**QP%**	**OA%**	**KA%**
Test area 1	KL-divergence	1.774	0.613	62.000	36.047	29.524	89.291	0.975
Test area 2	KL-divergence	0.105	0.163	85.955	90.530	78.866	91.145	0.992
Test area 3	KL-divergence	0.023	0.163	86.000	97.727	84.314	88.889	0.663

4. DISCUSSION

The proposed methodology performed to evaluate 3D building change detection from satellite and aerial photography confirm its effectiveness. Results of both generated DSMs and KL-divergence have detailed discussed in this section.

Interestingly, Table 1, showed that the Aerial-DSM has better accuracy in term of RMSE, especially for the (test area one which is equal to 0.2275m and test area three =0.1826m), than the satellite-DSM, for the same areas RMSE were (0.9399m and 0.4762m) respectively. Furthermore, it is clear that the Aerial-DSM have a better accuracy, this is because that the aerial images have a higher GSD resolution than satellite images which is 0.10m

and 0.50m respectively which in turn means that more detailed information about shape of the building with their edges are identified from aerial DSMs than the satellite-DSMs.
On the other hand, table (4) records best result for test area 3 as the overall accuracy was 88.88 %. It is obvious that KLD algorithms was able to detect the changed buildings and constructed geometrical building shapes close to the original shapes. However, in the object based assessment method the changed buildings are treated as single objects without consideration of their shape and size. Moreover, an overall accuracy of (89.291%, 91.145% and 88.889 %) are achieved for test areas 1, 2 and 3 respectively. This in turn mean that KLD algorithm both can sufficiently distinguish between changed and unchanged buildings. However, when it has been compared with reference data it showed that are not sufficiently robust to be implemented alone. As in order to increase the accuracy and the rate of truly building change detection, further post-processing steps will need like removing unwanted error that may cause due to the DSM computation error and/or due to the different nature of the DSM sources.

5. CONCLUSION

This paper proposes an efficient algorithm for change detection in an urban area using different optical stereo datasets. The datasets are composed of multi-temporal DSMs extracted from aerial and satellite imagery. For detecting the changes, the KLD algorithm has been used. The KLD algorithm successfully detected all the height changes in the area, including the changes in the vegetation. To retain the buildings only, the NDVI index mask has been sued to remove the vegetation. Furthermore, the experiment results show that the mathematical morphology can be applied to improve the result by removing the false objects around the buildings that were produced due to vegetation mask submission and height subtraction. By comparing the result obtained from KLD with other methods such as (Pixle-Based image differencing), it can be noticed that the suggested method can achieve better results [22].
However, the algorithm mainly depends on the quality of the used DSMs and the building, in case the building's features are more accurate the errors will be less. Therefore, it is expected that the accuracy of change detection can be increased, in case a better stereo-matching algorithm is used for DSM generation such as Semi global matching.
It is also possible to extend the suggested algorithm to detect the changes caused due to disasters such as earthquake effects and forest changes since it depends on introducing the height in addition instead of radiometric information.

REFERENCES

1. Tian, J., 3D Change Detection from High and Very High Resolution Satellite Stereo Imagery. 2013, Universität Osnabrück-Germany.
2. Haverkamp, D.P., Rick. Change Detection Using Ikonos Imagery. in ASPRS 2003 Annual Conference Proceedings. 2003.
3. Chen, J., Peng,He, Chunyang Pu, Ruiliang, Shi, Peijun, Land-Use/Land-Cover Change Detection Using Improved Change-Vector Analysis. Photogrammetric Engineering & Remote Sensing, 2003. 69(4): p. 369-379 DOI: https://doi.org/10.14358/PERS.69.4.369.
4. Lu, D.M., P Brondizio, E Moran, Emilio, Change detection techniques. International journal of remote sensing, 2004. 25(12): p. 2365-2401 DOI: https://doi.org/10.1080/0143116031000139863.
5. Singh, A., Review Article Digital Change Detection Techniques Using Remotely-Sensed Data. International Journal of Remote Sensing, 1989. 10(6): p. 989-1003 DOI: https://doi.org/10.1080/01431168908903939.
6. Thomas Krauß, J.T., Automatic Change Detection from High-Resolution Satellite Imagery. Remote Sensing for Archaeology and Cultural Landscapes, 2020: p. 47-58 DOI: https://doi.org/10.1007/978-3-030-10979-0_4.
7. Mancino, G., Nolè, Angelo,Ripullone, Francesco,Ferrara, Agostino, Landsat TM Imagery and NDVI Differencing to Detect Vegetation Change: Assessing Natural Forest Expansion in Basilicata, southern

Italy. iForest-Biogeosciences and Forestry, 2014. 7(2): p. 75 DOI: doi: https://doi.org/10.3832/ifor0909-007.
8. Singh, A., Tropical Forest Monitoring Using Digital Landsat data in Northeastern India. 1984, University of Reading-England.
9. San, D.K.T., M. Automatic Building Detection and Delineation from High Resolution Space Images Using Model-Based Approach. in Proceedings of the ISPRS Workshop on Topographic Mapping from Space. 2006.
10. Choi, K., Lee, I ,Kim, S, A Feature Based Approach to Automatic Change Detection from Lidar Data in Urban Areas. Int. Arch. Photogramm. Remote Sens. Spat. Inf. Sci, 2009. 18: p. 259-264 DOI: https://doi.org/10.1080/2150704X.2016.1212418.
11. Jung, F., Detecting Building Changes from Multitemporal Aerial Stereopairs. ISPRS Journal of Photogrammetry and Remote Sensing, 2004. 58(3-4): p. 187-201 DOI: https://doi.org/10.1016/j.isprsjprs.2003.09.005.
12. Tian , C., Shiyong, Reinartz, Peter, Building Change Detection Based on Satellite Stereo Imagery and Digital Surface Models. IEEE Transactions on Geoscience and Remote Sensing, 2014. 52(1): p. 406-417 DOI: DOI:10.1109/TGRS.2013.2240692.
13. Varade, D., Change Detection of Buildings Using Satellite Images and DSM. 2011, Technical University of Munich
14. Huang, Y.C., Jiayi Li, An automatic change detection method for monitoring newly constructed building areas using time-series multi-view high-resolution optical satellite images. Remote Sensing Environment, 2020. 244 DOI: https://doi.org/10.1016/j.rse.2020.111802.
15. Konstantinidis, D., Building Detection for Monitoring of Urban Changes. 2017, Imperial College-London.
16. Jabari, S.R., Mohammad ,Fathollahi, Fatemeh,Zhang, Yun, Multispectral Change Detection Using Multivariate Kullback-Leibler Distance. ISPRS journal of Photogrammetry and Remote sensing, 2019. 147: p. 163-177 DOI: https://doi.org/10.1016/j.isprsjprs.2018.11.014.
17. Schenk, T., Digital photogrammetry: Vol. I: Background, fundamentals, automatic orientation produceres. 1999: TerraScience.
18. Belov, D.I. and R.D. Armstrong, Distributions of the Kullback–Leibler divergence with applications. British Journal of Mathematical and Statistical Psychology, 2011. 64(2): p. 291-309 DOI: https://doi.org/10.1348/000711010X522227.
19. Cui, S. and C. Luo, Feature-Based Non-Parametric Estimation of Kullback–Leibler Divergence for SAR Image Change Detection. Remote sensing letters, 2016. 7(11): p. 1102-1111 DOI: DOI:10.1080/2150704X.2016.1212418.
20. Hedberg, H., Image Processing Architectures for Binary Morphology and Labeling. 2008, Lund University-Sweden.
21. Liteanu, A., On the Design of an Image Processing Tool To Help Cell Enumeration, in Faculty of Computer Science. 2018, University of Namur-Belgium.
22. Sitav Hiwa, H.A., Dleen Mohammed, The use of pixel-based algorithm for automatic change detection of 3D Building from Aerial and Satellite Imagery: Erbil city as a case study. Zanco Journal of Pure and Applied Sciences, 2020. 32: p. 24-38 DOI: https://doi.org/10.21271/ZJPAS.32.2.4.